

Magnetically controllable attitude trajectory constructed using the particle swarm optimization method

Anna Okhitina^{a,*}, Dmitry Roldugin^b, Stepan Tkachev^c

^a *New Laboratory of Big Data and Intelligent Systems, Keldysh Institute of Applied Mathematics, Miusskaya sq., 4, Moscow, 125047, Russia, okhitina@phystech.edu*

^b *Space System Dynamics Department, Keldysh Institute of Applied Mathematics, Miusskaya sq., 4, Moscow, 125047, Russia, rolduginds@gmail.com*

^c *Space System Dynamics Department, Keldysh Institute of Applied Mathematics, Miusskaya sq., 4, Moscow, 125047, Russia, stevens_1@mail.ru*

* Corresponding Author

Abstract

Currently small satellites are very popular and valuable as a technology demonstration and educational missions, delivering new technologies and ideas into space as fast as possible. Small satellites missions may require mediocre accuracy, therefore active three-axis magnetic control system is well suited for the considered problem. However, the magnetic torque direction is restricted – it cannot be applied along the geomagnetic induction vector. This hinders local capability of the disturbance rejection. However, the induction vector changes its direction during the satellite motion along the orbit. The uncontrollable direction changes and all directions become available with time. This leads to general controllability of the attitude stabilization problem. The paper proposes specific control construction procedure. A cost function is suggested that ensures the calculated control torque direction close to the plane orthogonal to the geomagnetic induction vector. Since the cost function is not suitable for classical gradient optimization methods, non-gradient biologically inspired global optimization method – particle swarm optimization (PSO) – is utilized in the paper. First, PSO is used to construct an optimal magnetically controllable attitude trajectory. The control torque projection onto the geomagnetic induction vector is minimized. Second, the constructed torque is implemented using magnetorquers. Simulation also considers different disturbance factors. The resulting motion satisfies the given constraints and initial conditions. Overall, PSO method is used to construct a controllable trajectory, which is implemented with a magnetic attitude control system with a given accuracy.

Keywords: three-axis magnetic control, attitude control, particle swarm optimization, reference motion

1. Introduction

Small spacecraft (SC) are widely applicable today. They can be used either alone or in a group flight, which allows them to solve a large range of tasks. Small SC are usually made simple to keep cost down and simplify software development, while maintaining high reliability. Therefore, a magnetic attitude control system is often used, since it requires almost no energy consumption, and is also easy to manufacture. However, the control torque $\mathbf{M}_{magn} = \mathbf{m} \times \mathbf{B}_{magn}$ cannot be applied along the geomagnetic induction vector \mathbf{B}_{magn} . The direction of vector \mathbf{B}_{magn} changes during the satellite motion along the orbit and all directions become available with time. The system is generally controllable [1,2].

The problem of providing SC stabilization using only three-axis magnetic attitude control system proposed in [3,4] is widely considered now. The survey [5] describes in detail a large number of works on this topic. It is shown that the magnetic attitude control system is applicable not only in the simplest case (orbital stabilization, e.g.), but also in more complex modes. It is possible to obtain an accuracy of 8-12 degrees. In the paper [6], it is proposed to construct a control using the PD-controller and the

Floquet stability theory approach for choosing the optimal control gains. The resulting accuracy is about 10 degrees for this case. The paper [7] also discusses the problem of choosing optimal control coefficients. The method used in [6] is compared with the selection of control gains using the particle swarm optimization (PSO) method [8–10]. Stabilization accuracy in the case of simulation in an extended motion model (including a random disturbing torque) is 3 degrees. In addition, the work [11] describes the construction of 3-axis magnetic control strategy and corresponding flight tests. This is one of the few examples of successful on-board implementation of various operating modes using only the magnetic attitude control system (an attitude accuracy is 10-20 degrees).

In some missions, accuracy about 10 degrees may not be good enough, so this paper suggests an approach that can provide higher accuracy. Firstly, since there is a problem of local uncontrollability, there is no way to provide orbital stabilization with high accuracy. Therefore, it is proposed to construct magnetically controllable attitude trajectory in the vicinity of the equilibrium position in the orbital frame, that is, to ensure the minimum projection of the control torque onto the

application of PSO is described, and the result is presented. The third subsection is devoted to the problem of the necessary control gains search with the help of PSO. A formalized functional and results are also presented.

3.1 Particle swarm optimization

PSO is the algorithm of evolutionary optimization, which is based on the decision-making model by particles of the swarm [8–10]. Each particle p ($p = \overline{1, N}$, N is the number of particles in the swarm) at each generation i ($i = \overline{1, G}$, G is the maximum number of generations) has a certain position $\mathbf{x}_{p,i}$ and velocity $\mathbf{v}_{p,i}$. An optimization problem with the cost function $\Phi(\mathbf{x}_{p,i}): \mathbb{R}^D \rightarrow \mathbb{R}$ is posed for the swarm, where D is the number of problem parameters. Restrictions on parameter values are defined by the search space

$$\mathbb{U} = \left\{ \mathbf{x}_{p,i} \in \mathbb{R}^D \mid \eta_{low}^j \leq x_{p,i}^j \leq \eta_{up}^j, \right. \\ \left. j = \overline{1, D}, p = \overline{1, N}, i = \overline{1, G} \right\}.$$

The particle position determines a possible solution of the optimization problem. To find the best position each particle makes a decision about the direction of displacement at the next moment of time (next generation) based on its current velocity, it's best previous position and the best previous position among all particles:

$$\begin{aligned} \mathbf{x}_{p,i} &= \mathbf{x}_{p,i-1} + \mathbf{v}_{p,i}, \\ \mathbf{v}_{p,i} &= c_{in} \mathbf{v}_{p,i-1} + \\ &+ c_{cog} (\mathbf{x}_{best,p,i-1} - \mathbf{x}_{p,i-1}) + \\ &+ c_{soc} (\mathbf{x}_{local\ best,p,i-1} - \mathbf{x}_{p,i-1}). \end{aligned} \quad (3)$$

There are three components of the velocity in (3):

- $c_{in} \mathbf{v}_{p,i-1}$ is the *inertial component*, it is responsible for the search continuation in the same direction;
- $c_{cog} (\mathbf{x}_{best,p,i-1} - \mathbf{x}_{p,i-1})$ is the *cognitive component*, the desire to return to its own better position found earlier;
- $c_{soc} (\mathbf{x}_{local\ best,p,i-1} - \mathbf{x}_{p,i-1})$ is the *social component*, representing striving for a better position found in the vicinity – each particle p has information about n another particles (the case $n = N$ is possible).

The contribution of each velocity component varies with the help of corresponding weighting coefficients c_{in} , c_{cog} and c_{soc} . They can be selected in various ways [8]. In this paper the coefficients are defined as:

$$c_{in,i} = (c_{in}^{low} - c_{in}^{up}) \frac{i}{G} + c_{in}^{up}$$

$$c_{cog,i} = U(0, c_{cog}^{up}) \left((c_{cog}^{low} - c_{cog}^{up}) \frac{i}{G} + c_{cog}^{up} \right), \\ c_{soc,i} = U(0, c_{soc}^{up}) \left((c_{soc}^{up} - c_{soc}^{low}) \frac{i}{G} + c_{soc}^{low} \right),$$

where $U(a, b)$ are uniformly distributed random numbers, a is a lower endpoint (minimum), b is an upper endpoint (maximum), $c_{in}^{low} = 0.4$, $c_{in}^{up} = 0.9$, $c_{soc}^{low} = c_{cog}^{low} = 0$, $c_{soc}^{up} = c_{cog}^{up} = 2.05$. After calculating the velocity and position of the particle at the next moment in time, it is necessary to check whether the new position does not go beyond the search area:

$$\eta_{low}^j \leq x_{p,i}^j \leq \eta_{up}^j \\ 0.15 \cdot \eta_{low}^j \leq v_{p,i}^j \leq 0.15 \cdot \eta_{up}^j.$$

Otherwise, it is necessary to normalize them. The coefficient 0.15 is chosen here based on the results obtained in studies [10,12], which show that each element of the minimum or maximum velocity values must be limited by the corresponding range of the search space and should be 10-20% of this range, otherwise the particle can easily leave the search space already in the first generations. Then in this case, the process of an optimal solution searching will slow down.

Moreover, this work adopts an increasing size of the neighborhood by a unity after every $k = 20$ generations. The initial size of the neighborhood equals 4.

One consider that the swarm has found the best position and, therefore, the optimal problem solution, if at some iteration two search stop criteria are satisfied:

- the cost function derivative is small (cost function stagnation);
- all particles are falling into some neighborhood of the best position (swarm stagnation).

3.2 Search of the optimal trajectory

First of all, we should find special trajectory for SC. Magnetic attitude control system must maintain a given attitude.

The spacecraft in a circular orbit with an altitude of $h = 550$ km is considered. The orbital inclination is $i_{orb} = 57^\circ$, orbital period is $T_0 = 2\pi\sqrt{r^3/\mu} \approx 1.58$ h. The time step is $dt = 5$ s and the considered time interval is $t \in (0, T_0)$. The SC has the shape of a parallelepiped $10 \times 20 \times 30$ cm, the SC center of mass is displaced by 1 cm along the positive direction of the second axis in the satellite-fixed frame. The inertia tensor of the satellite is $\mathbf{J} = \text{diag}(0.15, 0.13, 0.11)$ kg · m².

At this stage, it is required to find a trajectory where the projection of the control torque \mathbf{M}_{ctrl} onto the Earth's geomagnetic induction vector \mathbf{B}_{magn} is minimal:

$$\Phi_1 = \frac{1}{T/dt} \sqrt{\sum_{t=t_0=0}^T \left(\frac{\mathbf{M}_{ctrl,t}}{|\mathbf{M}_{ctrl,t}|}, \frac{\mathbf{B}_{magn,t}}{|\mathbf{B}_{magn,t}|} \right)^2} \rightarrow \min.$$

In this case we use the direct dipole model to describe the geomagnetic field, [13]:

$$\mathbf{B}_{magn,t} = B_0 \begin{pmatrix} \cos u(t) \sin i_{orb} \\ \cos i_{orb} \\ -2 \sin u(t) \sin i_{orb} \end{pmatrix},$$

$\mathbf{B}_{magn,t}$ is the geomagnetic induction vector in the orbital frame, $B_0 = \mu_e / r^3$, $u(t) = \omega_0 t$ is dependence the argument of latitude on time.

Consider the angular trajectory in the form of periodic functions:

$$\begin{aligned} \alpha(t) &= a_1 \sin u(t) + a_2 \cos u(t) + \\ &\quad + a_3 \sin 2u(t) + a_4 \cos 2u(t), \\ \beta(t) &= b_1 \sin u(t) + b_2 \cos u(t) + \\ &\quad + b_3 \sin 2u(t) + b_4 \cos 2u(t), \\ \gamma(t) &= g_1 \sin u(t) + g_2 \cos u(t) + \\ &\quad + g_3 \sin 2u(t) + g_4 \cos 2u(t), \end{aligned} \quad (4)$$

where $a_1, a_2, a_3, a_4, b_1, b_2, b_3, b_4, g_1, g_2, g_3, g_4$ are the required optimal constants specifying the trajectory (will be found as a result of PSO).

The absolute angular velocity in terms of the entered angles (in this stage $\mathbf{A} = \mathbf{B}$, $\mathbf{D} = \mathbf{E} = \text{diag}(1, 1, 1)$, see Figs. 1, 2) is

$$\boldsymbol{\omega}_{abs}^{SF} = (\mathbf{A}(\boldsymbol{\omega}_0^{OF} + \boldsymbol{\omega}_{ref}^{OF}))^{SF} + \boldsymbol{\omega}_{rel}^{SF}, \quad (5)$$

where $\boldsymbol{\omega}_{rel}^{SF} = (0, 0, 0)$ – since we assume that the spacecraft is already on the trajectory, $\boldsymbol{\omega}_0^{OF} = (0, \omega_0, 0)$ is orbital angular velocity (constant vector in the OF),

$$\begin{aligned} \boldsymbol{\omega}_{ref}^{OF} &= \dot{\boldsymbol{\alpha}} + \dot{\boldsymbol{\beta}} + \dot{\boldsymbol{\gamma}} = \mathbf{j}_1 \dot{\alpha} + \mathbf{j}_2 \dot{\beta} + \mathbf{j}_3 \dot{\gamma} = \\ &= \begin{pmatrix} 0 \\ 1 \\ 0 \end{pmatrix} \dot{\alpha} + \begin{pmatrix} \sin \alpha \\ 0 \\ \cos \alpha \end{pmatrix} \dot{\beta} + \begin{pmatrix} \cos \alpha \cos \beta \\ \sin \beta \\ -\sin \alpha \cos \beta \end{pmatrix} \dot{\gamma}. \end{aligned} \quad (6)$$

As a result,

$$\boldsymbol{\omega}_{abs}^{SF} = \mathbf{A} \left(\begin{pmatrix} 0 \\ \omega_0 \\ 0 \end{pmatrix} + \begin{pmatrix} \dot{\beta} \sin \alpha + \dot{\gamma} \cos \alpha \cos \beta \\ \dot{\alpha} + \dot{\gamma} \sin \beta \\ \dot{\beta} \cos \alpha - \dot{\gamma} \sin \alpha \cos \beta \end{pmatrix} \right). \quad (7)$$

Similarly, the derivative of the angular velocity is

$$\dot{\boldsymbol{\omega}}_{abs}^{SF} = (\dot{\mathbf{A}}(\boldsymbol{\omega}_0^{OF} + \boldsymbol{\omega}_{ref}^{OF}))^{SF} + \dot{\boldsymbol{\omega}}_{rel}^{SF} + (\mathbf{A} \dot{\boldsymbol{\omega}}_{ref}^{OF})^{SF}. \quad (8)$$

Here $\dot{\boldsymbol{\omega}}_{rel}^{SF} = (0, 0, 0)$, $\dot{\boldsymbol{\omega}}_{ref}^{OF} = (\dot{\omega}_{1,ref}^{OF}, \dot{\omega}_{2,ref}^{OF}, \dot{\omega}_{3,ref}^{OF})$,

$$\dot{\mathbf{A}} = -[\boldsymbol{\omega}_{abs} - \mathbf{A}\boldsymbol{\omega}_0]_{\times} \mathbf{A},$$

$$\mathbf{W} = -[\boldsymbol{\omega}_{abs} - \mathbf{A}\boldsymbol{\omega}_0]_{\times} = -[\boldsymbol{\omega}]_{\times} = \begin{bmatrix} 0 & -\omega_3 & \omega_2 \\ \omega_3 & 0 & -\omega_1 \\ -\omega_2 & \omega_1 & 0 \end{bmatrix}$$

is the cross product matrix.

We express \mathbf{M}_{ctrl} from the equation (1) and then substitute the angular velocity (7), its derivative (8), and expressions for \mathbf{M}_{grav} and \mathbf{M}_{aero} as

$$\mathbf{M}_{ctrl} = \mathbf{J}\dot{\boldsymbol{\omega}}_{abs} + \boldsymbol{\omega}_{abs} \times \mathbf{J}\boldsymbol{\omega}_{abs} - \mathbf{M}_{grav} - \mathbf{M}_{aero}.$$

Here we consider the case when $\mathbf{M}_{dist} = (0, 0, 0)$, \mathbf{M}_{aero} is calculated as in the paper [14].

After all the necessary substitutions, we find that the control torque \mathbf{M}_{ctrl} is a function of 12 parameters. The optimal ones must be found using the PSO. The total number of particles is $N = 24$ (2 times more than the number of required parameters). Each particle has a 12-dimensional position vector in the search area:

$$\begin{aligned} \mathbf{x}_{p,i} &= (a_1, a_2, a_3, a_4, b_1, b_2, b_3, b_4, g_1, g_2, g_3, g_4), \\ D &= 12, N = 24, G = 100 \end{aligned}$$

Parameter constraints are as follows

$$\eta_{low}^j = -2^\circ, \eta_{up}^j = 2^\circ, j = \overline{1, D}, \eta \text{ stands for } a, b, \text{ and } g$$

The results of the algorithm operation are shown in Fig. 3, 4 and 5. Fig. 3 demonstrates the reference trajectory constructed using PSO method. The trajectory lies entirely in the interval $(-2^\circ, 2^\circ)$, which satisfies the given constraints. Fig. 4 shows the control torque projection onto the geomagnetic induction vector, which is calculated at each step of time t as follows:

$$\mathbf{M}_{ctrl,B,t} = \left(\frac{\mathbf{M}_{ctrl,t}}{|\mathbf{M}_{ctrl,t}|}, \frac{\mathbf{B}_{magn,t}}{|\mathbf{B}_{magn,t}|} \right).$$

And in the Fig. 5 we can see the required control torque. The parameters for the reference trajectory are

$$\begin{aligned} a_1 &= 1.016 \cdot 10^{-2} \text{ rad}, & b_1 &= -4.028 \cdot 10^{-3} \text{ rad}, \\ a_2 &= 2.545 \cdot 10^{-2} \text{ rad}, & b_2 &= -9.717 \cdot 10^{-3} \text{ rad}, \\ a_3 &= 1.449 \cdot 10^{-3} \text{ rad}, & b_3 &= -4.841 \cdot 10^{-5} \text{ rad}, \\ a_4 &= 1.124 \cdot 10^{-3} \text{ rad}, & b_4 &= 2.231 \cdot 10^{-4} \text{ rad}, \\ g_1 &= 8.067 \cdot 10^{-3} \text{ rad}, \\ g_2 &= -4.127 \cdot 10^{-3} \text{ rad}, \\ g_3 &= -2.433 \cdot 10^{-2} \text{ rad}, \\ g_4 &= -4.637 \cdot 10^{-4} \text{ rad}. \end{aligned} \quad (9)$$

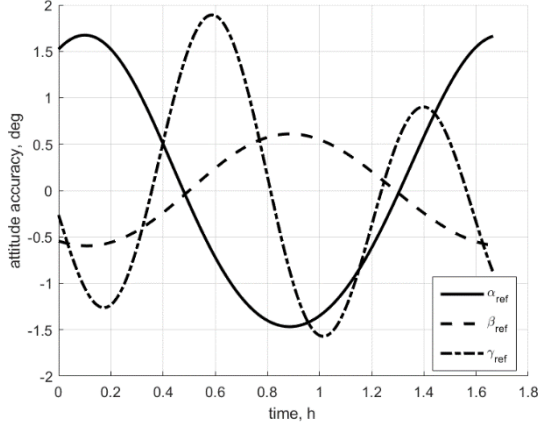


Fig. 3. Reference trajectory constructed using PSO

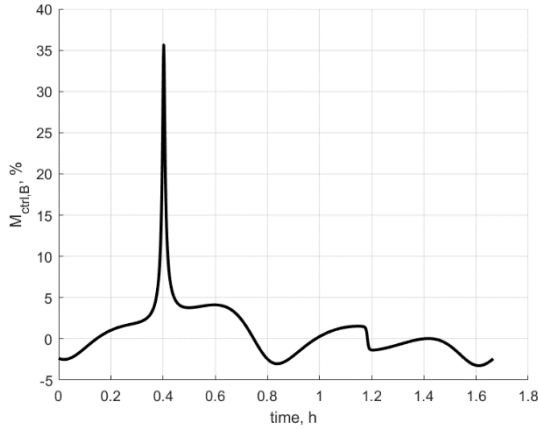


Fig. 4. Control torque projection onto the geomagnetic induction vector

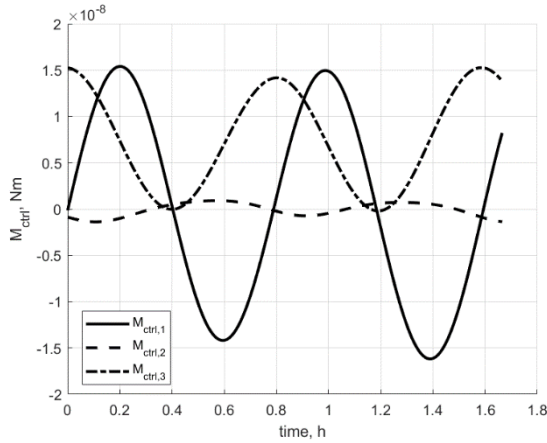


Fig. 5. Control torque \mathbf{M}_{ctrl}

One can see that the trajectory fully satisfies the given constraints, and the projection of the control torque onto the Earth's magnetic induction vector is about 5%. The peak on the chart in the Fig. 4 is explained by the fact that the absolute value of the control torque $|\mathbf{M}_{ctrl}|$ at this moment of time is close to zero (Fig. 5).

3.3 Selection of control gains

After obtaining the reference trajectory, it is necessary to construct a magnetic torque, which ensures convergence.

We rewrite the dynamic Euler equations (1) by substituting the derivative of the absolute angular velocity (8) (hereinafter, the indications of coordinate systems are omitted):

$$\mathbf{J}\left(\dot{\mathbf{A}}(\boldsymbol{\omega}_0 + \boldsymbol{\omega}_{ref})\right) + \dot{\boldsymbol{\omega}}_{rel} + \left(\mathbf{A}\dot{\boldsymbol{\omega}}_{ref}\right) + \boldsymbol{\omega}_{abs} \times \mathbf{J}\boldsymbol{\omega}_{abs} = \mathbf{M}_{grav} + \mathbf{M}_{aero} + \mathbf{M}_{ctrl},$$

Then

$$\mathbf{J}\dot{\boldsymbol{\omega}}_{rel} = \mathbf{M}_{grav} + \mathbf{M}_{aero} + \mathbf{M}_{ctrl} - \boldsymbol{\omega}_{abs} \times \mathbf{J}\boldsymbol{\omega}_{abs} - \mathbf{J}\left(\dot{\mathbf{A}}(\boldsymbol{\omega}_0 + \boldsymbol{\omega}_{ref})\right) - \mathbf{J}\left(\mathbf{A}\dot{\boldsymbol{\omega}}_{ref}\right). \quad (10)$$

To ensure asymptotic stability we will look for a Lyapunov function in the following form [15]:

$$V = \frac{1}{2}(\boldsymbol{\omega}_{rel}, \mathbf{J}\boldsymbol{\omega}_{rel}) + k_a((1-d_{11}) + (1-d_{22}) + (1-d_{33})),$$

$$k_a = const > 0,$$

then we get the expression for \dot{V} :

$$\begin{aligned} \dot{V} &= (\boldsymbol{\omega}_{rel}, \mathbf{J}\dot{\boldsymbol{\omega}}_{rel}) - k_a(\omega_{3,rel}(d_{21} - d_{21}) + \omega_{2,rel}(d_{13} - d_{31}) + \\ &+ \omega_{1,rel}(d_{32} - d_{23})) = (\boldsymbol{\omega}_{rel}, \mathbf{J}\dot{\boldsymbol{\omega}}_{rel}) + k_a(\boldsymbol{\omega}_{rel}, \mathbf{S}) = \\ &= (\boldsymbol{\omega}_{rel}, \mathbf{J}\dot{\boldsymbol{\omega}}_{rel} + k_a\mathbf{S}), \end{aligned}$$

where d_{ij} – the elements of the matrix \mathbf{D} (Fig. 2),

$$\mathbf{S} = \begin{pmatrix} d_{23} - d_{32} \\ d_{31} - d_{13} \\ d_{12} - d_{21} \end{pmatrix}, \quad \boldsymbol{\omega}_{rel} = \begin{pmatrix} \omega_{1,rel} \\ \omega_{2,rel} \\ \omega_{3,rel} \end{pmatrix}, \quad \text{and } k_a \text{ is a positive}$$

coefficient, $[k_a] = [\text{N} \cdot \text{m}]$.

To satisfy the Barbashin-Krasovskiy theorem, the derivative of the candidate Lyapunov function must be non-positive due to the equations of motion. So, we require that

$$\mathbf{J}\dot{\boldsymbol{\omega}}_{rel} + k_a\mathbf{S} = -k_{\omega}\boldsymbol{\omega}_{rel}, \quad k_{\omega} = const > 0. \quad (11)$$

Taking into account (10) and (11) the expression for the control torque can be written in the form:

$$\mathbf{M}_{ctrl} = -k_{\omega}\boldsymbol{\omega}_{rel} - k_a\mathbf{S} + \boldsymbol{\omega}_{abs} \times \mathbf{J}\boldsymbol{\omega}_{abs} + \mathbf{J}\dot{\mathbf{A}}(\boldsymbol{\omega}_0 + \boldsymbol{\omega}_{ref}) + \mathbf{J}\mathbf{A}\dot{\boldsymbol{\omega}}_{ref} - \mathbf{M}_{grav} - \mathbf{M}_{aero} \quad (12)$$

In this case we find that the control torque \mathbf{M}_{ctrl} depends in two 2 control parameters k_a, k_{ω} . The optimal ones also must be found using the PSO, substituting the values for the reference trajectory found at the previous stage (9).

However, in contrast to the previous case, the control torque \mathbf{M}_{ctrl} cannot be calculated directly, since it depends on the phase variables which must be obtained by integrating the equations of motion (2). Integration

step and control step are $dt = 5 \text{ s}$. For numerical integration, the Runge-Kutta 4th order method is used.

It is important to note that only the component of the control torque, which is not directed along the vector of the Earth's geomagnetic induction, should be substituted into (2) when integrating. So the control torque applied by magnetorquers is

$$\mathbf{M}_{\text{magn}} = \mathbf{m} \times \mathbf{B}_{\text{magn}},$$

where $\mathbf{m} = \frac{\mathbf{B}_{\text{magn}} \times \mathbf{M}_{\text{ctrl}}}{B_{\text{magn}}^2}$ is SC dipole moment, see Fig. 6.

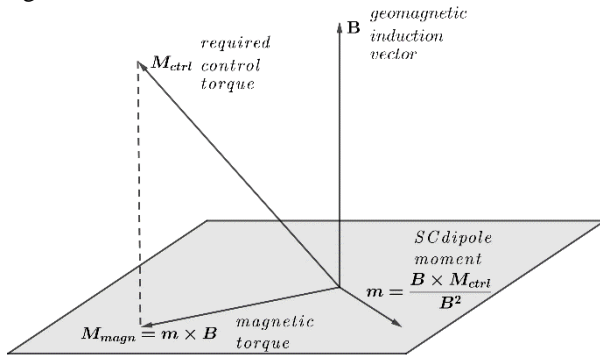


Fig. 6. Obtaining a magnetic control torque

Now we can set an optimization problem for the swarm in this case. The coefficients k_a , k_ω must be strictly greater than 0, so we choose the cost function by finding the derivative of Φ_1 taking into account the expression for the control torque (12):

$$\Phi_2 = \left(\sum_{t=t_0=0}^T \left((\boldsymbol{\omega}_{\text{rel},t}^T \mathbf{B}_{\text{magn},t}) \cdot (\mathbf{M}_{\text{ctrl},t}^T \mathbf{B}_{\text{magn},t}) \right)^2 + \sum_{t=t_0=0}^T \left((\mathbf{S}_t^T \mathbf{B}_{\text{magn},t}) \cdot (\mathbf{M}_{\text{ctrl},t}^T \mathbf{B}_{\text{magn},t}) \right)^2 \right) \rightarrow \min.$$

Parameters for the PSO method in this case:

$$\mathbf{x}_{p,i} = (k_a, k_\omega), \quad D = 2, \quad N = 12, \quad G = 100$$

Its restrictions:

$$\eta_{\text{low}}^1 = \eta_{k_a, \text{low}} = 10^{-8}, \quad \eta_{\text{up}}^1 = \eta_{k_a, \text{up}} = 5 \cdot 10^{-5},$$

$$\eta_{\text{low}}^2 = \eta_{k_\omega, \text{low}} = 5 \cdot 10^{-5}, \quad \eta_{\text{up}}^2 = \eta_{k_\omega, \text{up}} = 10^{-2}.$$

The search for the coefficients is carried out under the assumption that the initial data of the spacecraft coincide with the initial data of the reference trajectory $\alpha_0, \beta_0, \gamma_0$ and angular velocity $\boldsymbol{\omega}_{\text{init}}$, which can be obtained by substituting the found parameters of the trajectory (9) into the expressions (4) and (6).

As a result, the coefficients (control gains) found by the PSO are $k_a = 6.578 \cdot 10^{-8}$, $k_\omega = 1.119 \cdot 10^{-4}$.

Figs. 7-12 represent simulating results.

So, the trajectory found at the first stage is successfully implemented by the magnetic control obtained at the second stage. Thus, we constructed magnetically controllable attitude trajectory using PSO method.

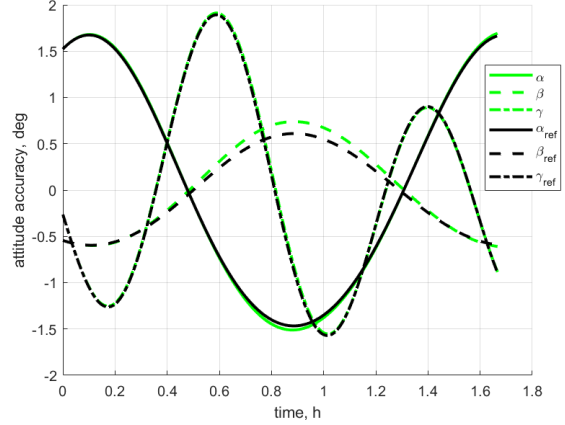


Fig. 7. Reference and real trajectory

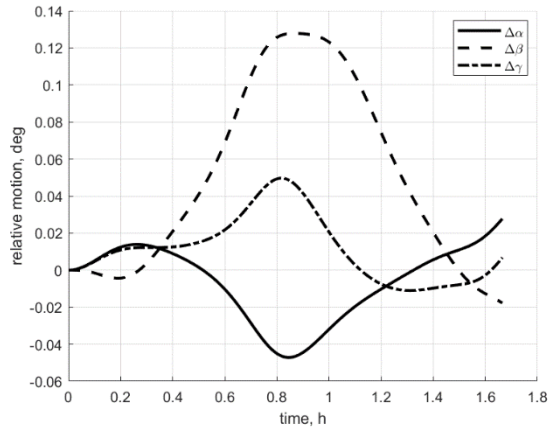


Fig. 8. Reference trajectory deviation

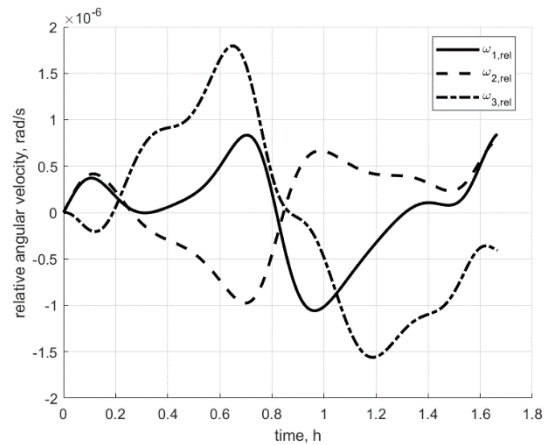


Fig. 9. Relative angular velocity

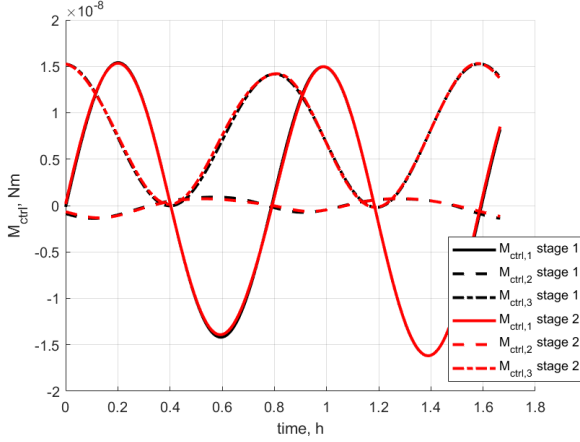


Fig. 10. Control torque \mathbf{M}_{ctrl} for each of two stages

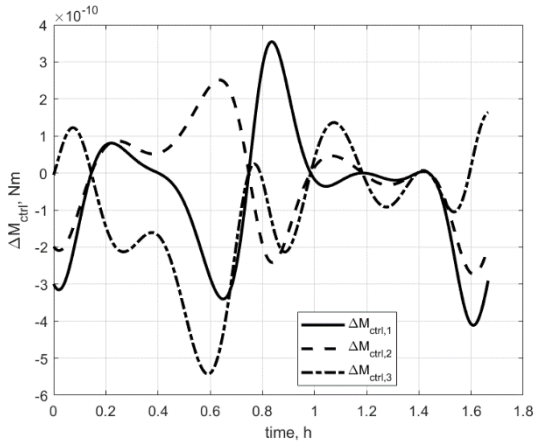


Fig. 11. The difference between the required control torque \mathbf{M}_{ctrl} and the realized one \mathbf{M}_{magn}

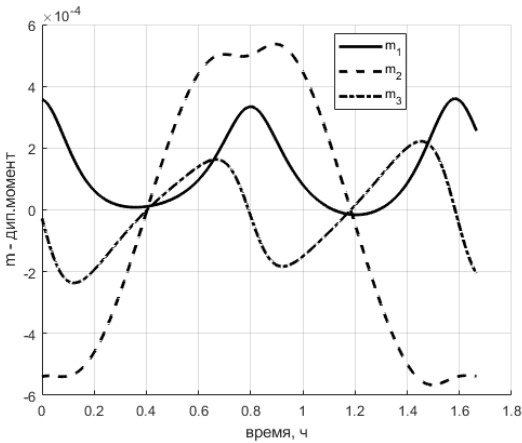


Fig. 12. SC dipole moment

4. Numerical simulation and results

The extended model with various disturbances and the inaccuracy of knowledge of SC initial conditions is considered for the numerical simulation and algorithm operation illustration. The three-axis magnetic attitude control system should ensure SC stabilization on a given

trajectory. Parameters and data used in this case are presented in the Table 1. In the simulation the inclined dipole model is used.

Table 1. Parameters for numerical simulation

Name	Value
Simulation time	$t \in (0, T)$ $T = 20T_0 \approx 33$ h,
SC initial angular velocity	$\boldsymbol{\omega} = 10 \cdot \boldsymbol{\omega}_{mir}$ rad/s
SC initial orientation	$\alpha = \alpha_0 + 10^\circ \cdot \frac{\pi}{180^\circ}$ rad $\beta = \beta_0 + 10^\circ \cdot \frac{\pi}{180^\circ}$ rad $\gamma = \gamma_0 + 10^\circ \cdot \frac{\pi}{180^\circ}$ rad
Magnetic field model	inclined dipole, [13]
Inaccuracy of knowledge of the density of the atmosphere	20%
External random disturbances	$\mathbf{M}_{dist} = 10^{-9} \cdot \mathbf{k}_{dist}$, \mathbf{k}_{dist} is normally distributed random vector, $k_{i,dist} \in [0, 1]$, $i = 1, 3$

The results are shown in Figs. 13-18.

One can see that the real trajectory differs from the reference one by 1-2 degrees (Fig. 13-14). However, the specified constraints are still met (stabilization accuracy ± 1 degrees in steady state). The deviation of the reference trajectory decreases with time and in the steady state it remains at the same level for an arbitrarily long time (the simulation can be continued for more than 20 turns), which indicates the stability of the resulting motion.

The control torque realized by the magnetic attitude control system \mathbf{M}_{magn} also differs from the calculated one (Fig. 16). In this case, it can be seen that in steady state the difference between the required control torque \mathbf{M}_{ctrl} and the realized one \mathbf{M}_{magn} is about 10^{-9} N·m (Fig. 17), which is about 10-20% of the absolute value of the required control torque. This means that 80-90% of \mathbf{M}_{ctrl} can always be realized. In general, it is possible to ensure the controllability of the SC, while satisfying the specified constraints on the attitude accuracy.

Eventually the results of numerical simulation indicate that such control torque is effective even in the presence of external disturbances not taken into account, such as inaccuracy in the knowledge of the initial conditions, the atmosphere model or the presence of random disturbances.

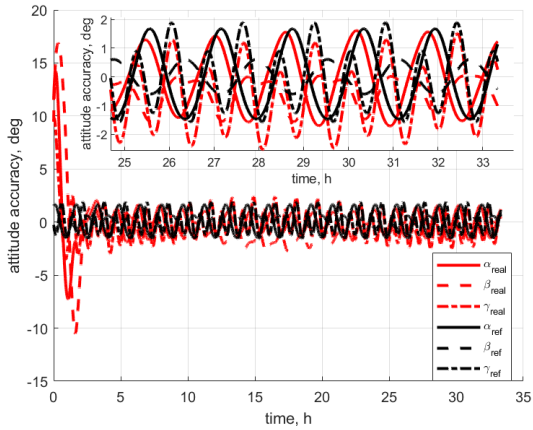


Fig. 13. Reference and real trajectory

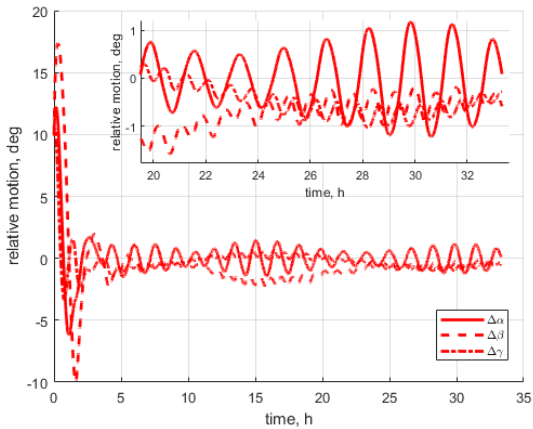


Fig. 14. Reference trajectory deviation

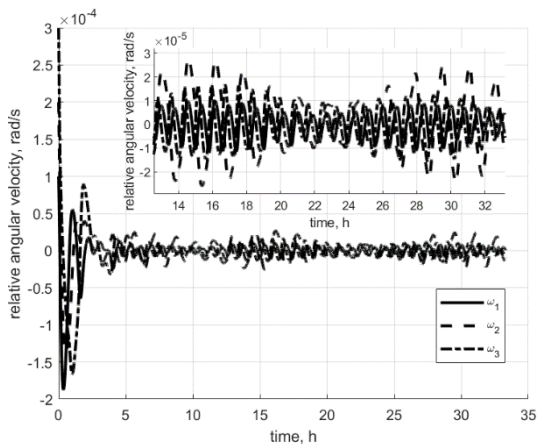


Fig. 15. Relative angular velocity

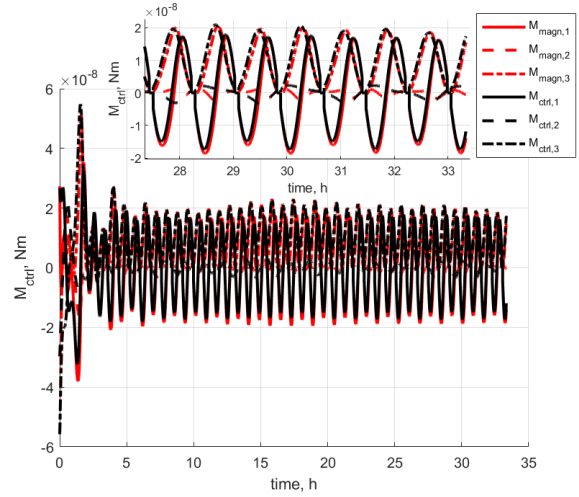


Fig. 16. Control torque M_{ctrl} and magnetic torque M_{magn}

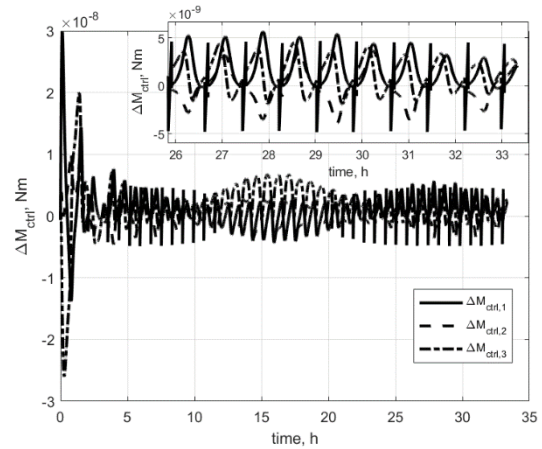


Fig. 17. The difference between the required control torque M_{ctrl} and the realized one M_{magn}

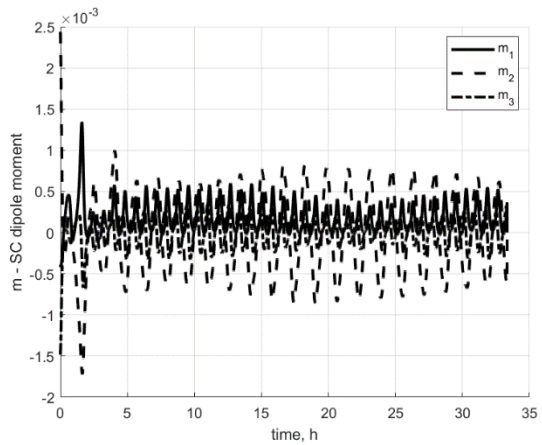


Fig. 18. SC dipole moment

5. Conclusions

The article proposes a method for constructing an angular trajectory, which is fully realizable by a magnetic attitude control system. It is shown how the particle swarm optimization method is applied to find the optimal trajectory coefficients. The trajectory with the minimum control torque projection on geomagnetic induction vector is constructed. Then, the control gains are obtained using the Lyapunov function approach to ensure asymptotic stability. Optimal control gains are also found using the PSO method adapted for this case. Finally, numerical simulation is carried out. It is shown that all the constraints are satisfied in the extended model as well. The orientation accuracy is about 2 degrees.

Acknowledgements

This work was supported by the Russian Science Foundation, project no 17-71-20117.

References

- [1] Bhat S.P. Controllability of nonlinear time-varying systems: applications to spacecraft attitude control using magnetic actuation // *IEEE Trans. Automat. Contr.* 2005. Vol. 50, № 11. P. 1725–1735.
- [2] Morozov V.M., Kalenova V.I. Satellite Control Using Magnetic Moments: Controllability and Stabilization Algorithms // *Cosm. Res.* Springer, 2020. Vol. 58, № 3. P. 158–166.
- [3] Lovera M., Astolfi A. Spacecraft attitude control using magnetic actuators // *Automatica*. 2004. Vol. 40, № 8. P. 1405–1414.
- [4] Wisniewski R., Blanke M. Fully magnetic attitude control for spacecraft subject to gravity gradient // *Automatica*. Pergamon, 1999. Vol. 35, № 7. P. 1201–1214.
- [5] Ovchinnikov M.Y., Roldugin D.S. A survey on active magnetic attitude control algorithms for small satellites // *Prog. Aerosp. Sci.* Pergamon, 2019. article 100546.
- [6] Ovchinnikov M.Y. et al. Choosing control parameters for three axis magnetic stabilization in orbital frame // *Acta Astronaut.* 2015. Vol. 116. P. 74–77.
- [7] Okhitina A.S., Roldugin D.S., Tkachev S.S. Biologically inspired optimization algorithm in satellite attitude control problems // *15th International Conference on Stability and Oscillations of Nonlinear Control Systems*. Moscow, 2020.
- [8] Simon D. *Evolutionary Optimization Algorithms*. WILEY, 2013. 742 p.
- [9] Kennedy J., Eberhart R. Particle swarm optimization // *Proceedings of International Conference on Neural Networks*. IEEE, 1995. Vol. 4. P. 1942–1948.
- [10] Eberhart R., Shi Y. Particle swarm optimization: Developments, applications and resources. // *IEEE Congr. Evol. Comput.* Seoul, Korea., 2001. P. 81–86.
- [11] Chasset C. et al. 3-Axis magnetic control: flight results of the TANGO satellite in the PRISMA mission // *CEAS Sp. J.* Springer Vienna, 2013. Vol. 5, № 1–2. P. 1–17.
- [12] Eberhart R., Shi Y. Comparing inertia weights and constriction factors in particle swarm optimization. // *IEEE Congr. Evol. Comput.* San Diego, Calif. 2000. P. 84–88.
- [13] Ovchinnikov M.Y. et al. Geomagnetic field models for satellite angular motion studies // *Acta Astronaut.* 2018. Vol. 144. P. 171–180.
- [14] Guerman A.D. et al. Orbital and Angular Dynamics Analysis of the Small Satellite SAR Mission INFANTE // *Cosm. Res.* 2020. Vol. 58, № 3. P. 206–217.
- [15] Ovchinnikov M.Y., Tkachev S.S., Karpenko S.O. A Study of Angular Motion of the Chibis-M Microsatellite with Three-Axis Flywheel Control // *Cosm. Res.* 2012. Vol. 50, № 6. P. 431–440.